Terahertz metamaterials on flexible polypropylene substrate

Rubén Ortuño[*1], Carlos García-Meca[2], and Alejandro Martínez[2]

[1]*TERALAB (MmW - THz – IR & Plasmonics Laboratory), Universidad Pública de Navarra, 31006, Pamplona, Spain*

[2]*Nanophotonics Technology Center (NTC), Universitat Politecnica de Valencia, Camino de Vera s/n, 46022, Valencia, Spain*

Phone: +34 96 387 97 68

Fax: +34 96 387 78 27

E-mail: ruben.ortuno@unavarra.es

URL: http://www.csm.unavarra.es

Abstract. In this work, we present a metamaterial working at terahertz frequencies made over a flexible polypropylene substrate. The experimental measurements, in accordance with the numerical calculations, show the metamaterial reliance on the impinging electric field polarization. The structure's symmetry yields purely electrical resonant responses eliminating bianisotropy effects. The widely used bendable polypropylene polymer may promote the insertion of metamaterial-based structures with special electromagnetic response in a number of objects of our daily lives such as textiles, automotive components, and sensing.

Keywords: Surface plasmon polaritons; Metamaterials; Terahertz; Polypropylene

Introduction

Metamaterials allow us to obtain electromagnetic responses not found in nature by free tuning both their permeability and permittivity effective parameters. Owing to this fascinating behaviour, metamaterials have attracted a wide interest as they offer great opportunities to be used in novel applications. For instance, metamaterials have brought about the possibility of realizing negative-index materials (NIMs) [1]. Additional relevant breakthroughs encompass superlenses surpassing the diffraction limit [2,3], invisibility cloaks for hiding an object from detection [4,5], and highly sensitive biosensors [6-8].

Although metamaterials can be engineered to fit almost any working spectral regime, metamaterial research has been mainly devoted to designing nanostructures for the visible range, where the fabrication is challenging. However, metamaterials are also of particular interest in other frequency regions. Particularly, the intense emerging interest in terahertz (THz) radiation, in addition to the dearth of naturally existing materials that can control THz waves, reinforces the interest on developing metamaterials at such frequencies. Thus, as opposed to the weak electric and magnetic responses exhibited by natural materials, metamaterials can be used as the building blocks of THz devices that cannot be realized with conventional materials. It is only recently that THz applications have been developed to fill the so-called THz gap. The state of the art includes absorbers [9-12], modulators [13-18], and molecular sensors [19-21].

On the other hand, traditional fabrication techniques typically require rigid substrates. Such a constraint limits the implementation of several applications, e.g. superlenses and cloaking devices for which a curved realization is desirable. Therefore, developing a technique that would allow the implementation of a curved topology will not only improve the metamaterial performance and its employability on multiple scenarios. It would also enable metamaterials to benefit from the growing field of transformation optics [22], where a full control of the refractive index in three axes over a defined volume is mandatory. In this sense, recent advances on metamaterials fabrication over mechanically flexible and transparent to THz radiation substrates have been demonstrated, providing a promising path to create non-planar metamaterials at THz frequencies [16-18,23-31].

In this work, we report on the fabrication and characterization of plasmonic metamaterial structures on flexible polypropylene (PP) substrates and demonstrate their optical properties at THz frequencies. The choice of PP is due to the advantages it presents among other polymer substrates. PP is a thermoplastic polymer normally tough and flexible. These properties, along with its resistance to fatigue and low cost, allow PP to be used in a wide variety of applications including packaging and labeling, textiles, automotive components and sensing. Moreover, its low dispersion and small dielectric losses within a very wide frequency range make PP a suitable polymer substrate for metamaterial applications [31].

Fabrication and measurement

A lift-off technique was employed to produce the flexible metamaterial depicted in Fig. 1(a), which comprises the periodical repetition of the unit cell shown in Fig. 1(b) until covering an area of 4 mm x 4 mm. First, the PP sample is mounted on a silicon wafer to allow an automatic process, rinsed with acetone and IPA in a spinner and dried at 110 ºC in a hot plate. Then the sample is spin-coated with a photoresist (Shipley S1818) to a 2 µm thick layer and baked at 115 ºC. Next, the resist is exposed in an EVG 620 mask-aligner with a dose of 150 mJ/cm2 and developed using a TMAH solution. At this point, the structure is checked before further processing. After this, metallization is carried out with an electron-beam PVD tool, which ensures normal evaporation and allows good profiles. Two metallic layers are deposited; first a 3 nm thick layer of chromium to improve the adherence and then the 30 nm thick gold layer. Finally, a lift-off step is done in hot NMP, and the sample is cleaned with IPA and dried with N_2. To show the quality of the fabrication process, optical microscope and SEM images are depicted in Fig. 1(c) and 1(d), respectively.

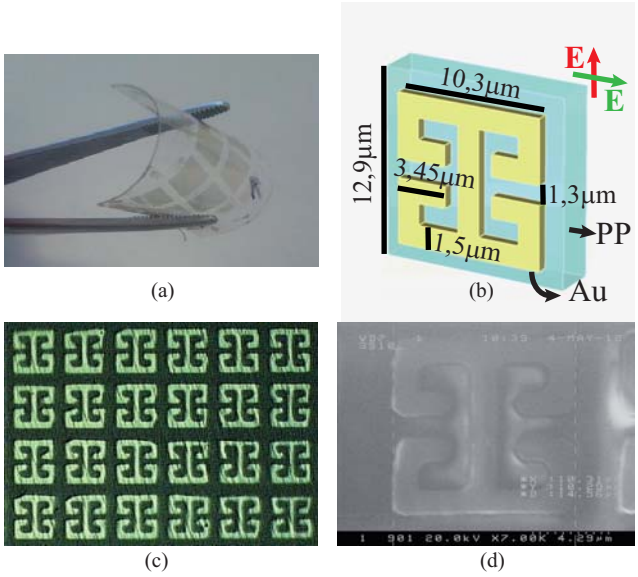

Fig. 1 (a) Photograph of the metamaterial fabricated over a flexible PP substrate. (b) Representation of the metamaterial's unit cell with the dimensions considered for the fabrication along with the two main polarization directions of the impinging electric field. (c) Optical microscope image of the fabricated metamaterial and (d) SEM image of the fabricated metamaterial's unit cell

For the optical characterization of the fabricated sample, transmission measurements were carried out using a Bruker Vertex 80 Fourier transform infrared (FTIR) spectroscopy system. Due to the technological constraints imposed by the equipment, it was not possible to measure the reflection spectrum. A polarized mercury-arc lamp source beam illuminates the fabricated subwavelength structures. The transmitted light is collected with a liquid nitrogen and helium cooled Bolometer detector coupled to the FTIR spectrometer to measure the transmission spectra of the sample. In the measurements, the sample was probed at normal incidence, ensuring that the electric and magnetic fields are configured to be completely in-plane. Hence, no component of the magnetic field is capable of causing a magnetic response by driving circulating currents. The

effect of curvature on the sample response is beyond the scope of this work, and will be addressed in forthcoming publications.

Discussion

To verify the results, we performed several numerical calculations with CST Microwave Studio. A refractive index of n = 1.5 was considered for PP, while the dispersive properties of gold were taken into account by using a Drude model with plasma frequency ω_p = 1.37e16 rad/s and collision frequency γ = 8.5e13 rad/s.

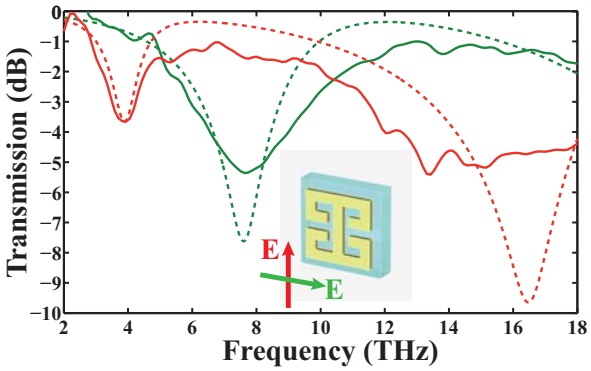

Fig. 2 Transmission measurements (plain) and simulations (dashed) for both vertical (red) and horizontal (green) electric field polarization

Both the co- and the cross-polar polarizations (electric field oriented, respectively, in the vertical and horizontal direction, as shown in the inset of Fig. 2) are considered in simulations and measurements. The good agreement between the experimental and numerical results (see Fig. 2) allows us to interpret the origin of the resonances from the simulations. The slight differences arise from fabrication tolerances and possible additional losses not taken into account by the simulation model. In addition, both the experimental and the numerical curves were normalized with respect to the transmission of a PP layer without the gold patterns to remove the oscillations due to Fabry-Perot resonances at the PP interfaces. All the observed resonances, with the transmission reaching values as low as -5 dB, have a purely electrical origin. The reason is that the symmetry of the structure makes the particle exhibit a resonant response to the electric field, while eliminating any magneto-electric coupling effects related to bianisotropy [32].

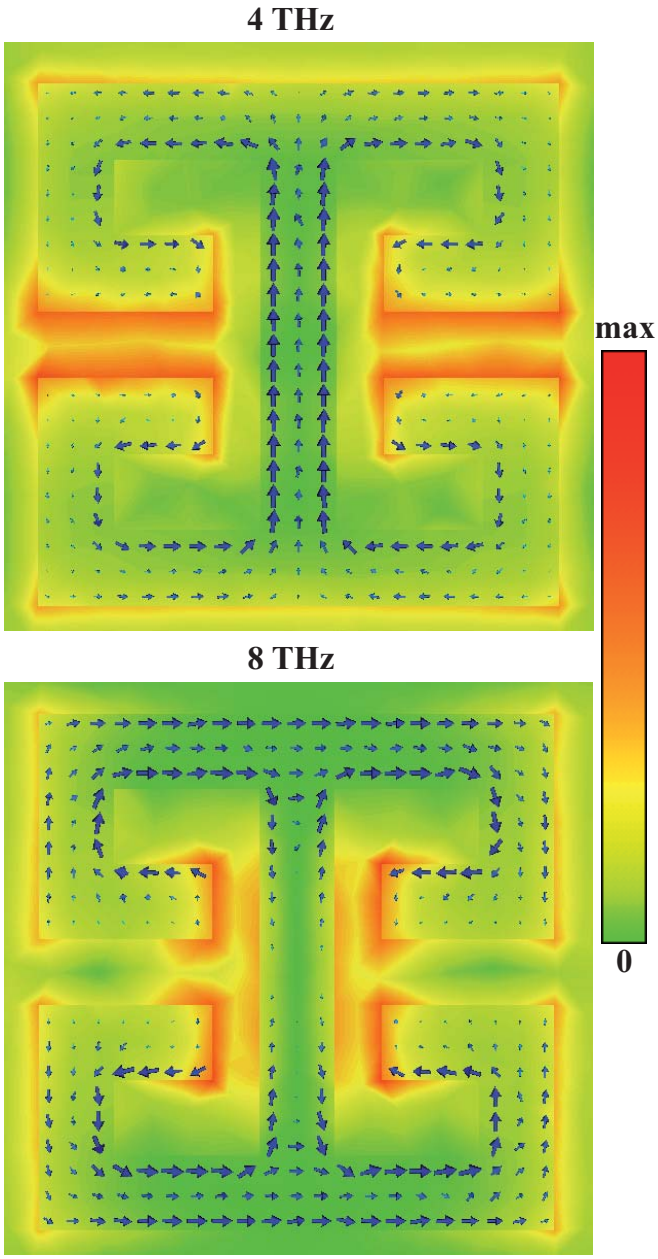

Fig. 3 Numerical simulation results for the co-polar resonances at 4THz (up) and cross-polar resonance at 8THz (down). The arrows indicate the induced surface current density and the color represents the electric field norm. The incident field is oriented as indicated in Fig. 1(b)

To visualize the absence of a magnetic response, the surface current densities at the co- and cross-polar resonances, 4 THz and 8 THz, respectively, are shown in Fig. 3. The incident electric field drives, at both resonances, clockwise and counterclockwise circulating surface currents in adjacent regions of the particle. Consequently, any magnetic particle's response is avoided, since there is no net current circulation in a unit cell. Hence, the particle's symmetry holds responsible for its resonant response to the electrical component of the impinging electromagnetic field. In addition, because of the charge accumulation at the capacitive gaps, the electric field is resonantly enhanced in their vicinity, as demonstrated by the distribution of the norm of the electric field represented in Fig. 3. Obviously, the lack of fourfold symmetry provokes the particle to exhibit a different electric response under a rotation of the incoming electric field. To verify this, angular measurements were performed by rotating the impinging electric

field from the horizontal to the vertical orientation. Figure 4 shows the evolution of the metamaterial response from the cross- to the co-polar behaviour with the angle that defines the electric field orientation. Note the good agreement between measurements and simulations. It should be mentioned that for the high-frequency resonance around 16 THz, which originates from the excitation of electric dipoles similar to that in cut wires [33], the structure is no longer in the effective medium regime.

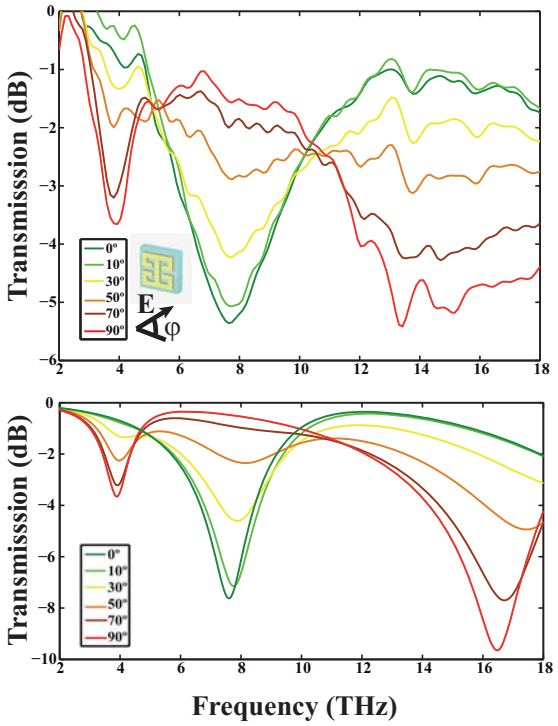

Fig. 4 Experimental (up) and numerical (down) transmission through the flexible metamaterial layer as a function of the electric field polarization's angle

Conclusions

In this paper, we have presented the fabrication of THz metamaterials over flexible polypropylene substrates with standard lithographic methods. The transmission measurements carried in the THz range (2-18 THz) exhibit a polarization-sensitive response. This behaviour was also checked numerically. The particles' symmetry makes them function as purely electrical resonant structures with a localized field extent, since the response derives from the individual unit cells. This design, in addition, facilitates the fabrication process, since no inter-unit cell connections are needed to obtain an electric response, such as in wire arrays. This feature makes the extension to higher dimensions straightforward, as in the case of structures based on split ring resonators [34].

Moreover, the results show the suitability of polypropylene as a flexible substrate to host metamaterial structures. Building THz metamaterials on flexible substrates makes them ideal building blocks for future generations of three-dimensional metamaterials and, opens a path to incorporate metamaterial devices on multiple scenarios, removing the limitations of conventional rigid substrates.

Acknowledgements This work was supported by the Spanish MICINN under contracts CONSOLIDER EMET CSD2008-00066 and TEC2011-28664-C02-02 and by the Universitat Politècnica de València under the programme INNOVA 2011.

References

[1] Smith DR, Padilla WJ, Vier DC, Nemat-Nasser SC, Schultz S (2000) Composite medium with simultaneously negative permeability and permittivity. Phys. Rev. Lett. 84:4184-4187

[2] Pendry JB (2000) Negative refraction makes a perfect lens. Phys. Rev. Lett. 85:3966-3969

[3] Zhang X, Liu Z (2008) Superlenses to overcome the diffraction limit. Nat. Mater. 7:435-441

[4] Pendry JB, Schurig D, Smith DR (2006) Controlling Electromagnetic Fields. Science 312:1780-1782

[5] Schurig D, Mock JJ, Justice BJ, Cummer SA, Pendry JB, Starr AF, Smith DR (2006) Metamaterial electromagnetic cloak at microwave frequencies. Science 314:977-980

[6] Rodríguez-Cantó PJ, Martínez-Marco M, Rodríguez-Fortuño FJ, Tomás-Navarro B, Ortuño R, Peransí-Llopis S, Martínez A (2011) Demonstration of near infrared gas sensing using gold nanodisks on functionalized silicon. Opt. Express 19:7664-7672

[7] Rodríguez-Fortuño FJ, Martínez-Marco M, Tomás-Navarro B, Ortuño R, Martí J, Martínez A, Rodríguez-Cantó PJ (2011) Highly-sensitive chemical detection in the infrared regime using plasmonic gold nanocrosses. Appl. Phys. Lett. 98:133118

[8] O'Hara FJ, Singh R, Brener I, Smirnova E, Han J, Taylor AJ, Zhang W (2008) Thin-film sensing with planar terahertz metamaterials: sensitivity and limitations. Opt. Express 16:1786-1795

[9] Tao H, Landy NI, Bingham CM, Zhang X, Averitt RD, Padilla WJ (2008) A metamaterial absorber for the terahertz regime: design, fabrication and characterization. Opt. Express 16:7181-7188

[10] Iwaszczuk K, Strikwerda AC, Fan K, Zhang X, Averitt RD, Jepsen PU (2012) Flexible metamaterial absorbers for stealth applications at terahertz frequencies. Opt. Express 20:635-643

[11] Tao H, Bingham CM, Strikwerda AC, Pilon D, Shrekenhamer D, Landy NI, Fan K, Zhang X, Padilla WJ, Averitt RD (2008) Highly flexible wide angle of incidence terahertz metamaterial absorber: Design, fabrication, and characterization. Phys. Rev. B 78:241103(R)

[12] Tao H, Bingham CM, Pilon D, Fan K, Strikwerda AC, Shrekenhamer D, Padilla WJ, Zhang X, Averitt RD (2010) A dual band terahertz metamaterial absorber. J. Phys. D: Appl. Phys. 43:225102

[13] Padilla WJ, Taylor AJ, Highstrete C, Lee M, Averitt RD (2006) Dynamical electric and magnetic metamaterial response at terahertz frequencies. Phys. Rev. Lett. 96:107401

[14] Chen HT, Padilla WJ, Zide JMO, Gossard AC, Taylor AJ, Averitt RD (2006) Active terahertz metamaterial devices. Nature 444:597-600

[15] Chen HT, O'Hara FJ, Azad AK, Taylor AJ, Averitt RD, Shrekenhamer DB, Padilla WJ (2008) Experimental demonstration of frequency-agile terahertz metamaterials. Nature Photon. 2:295-298

[16] Chen HT, Padilla WJ, Zide JMO, Bank SR, Gossard AC, Taylor AJ, Averitt RD (2007) Ultrafast optical switching of terahertz metamaterials fabricated on ErAs/GaAs nanoisland superlattices. Opt. Lett. 32:1620-1622

[17] Chen HT, Palit S, Tyler T, Bingham CM, Zide JMO, O'Hara FJ, Smith DR, Gossard AC, Averitt RD, Padilla WJ, Jokerst NM, Taylor AJ (2008) Hybrid metamaterials enable fast electrical modulation of freely propagating terahertz waves. Appl. Phys. Lett. 93:091117

[18] Chen HT, Padilla WJ, Cich MJ, Azad AK, Averitt RD, Taylor AJ (2009) A metamaterial solid-state terahertz phase modulator. Nat. Photon. 3:148

[19] Driscoll T, Andreev GO, Basov DN, Palit S, Cho SY, Jokerst NM, Smith DR (2007) Tuned permeability in terahertz split-ring resonators for devices and sensors. Appl. Phys. Lett. 91:062511

[20] Debus C, Bolivar PH (2007) Frequency selective surfaces for high sensitivity terahertz sensing. Appl. Phys. Lett. 91:184102

[21] Al-Naib IAI, Jansen C, Koch M (2008) Thin-film sensing with planar asymmetric metamaterial resonators. Appl. Phys. Lett. 93:083507

[22] Leonhardt U, Philbin TG (2010) Geometry and Light: The Science of Invisibility. Mineola, NY: Dover

[23] Di Falco A, Ploschner M, Krauss TF (2010) Flexible metamaterials at visible wavelengths. New J. Phys. 12:113006

[24] Tao H, Strikwerda AC, Fan K, Bingham CM, Padilla WJ, Zhang X, Averitt RD (2008) Terahertz metamaterials on free-standing highly-flexible polyimide substrates. J. Phys. D, Appl. Phys. 41:232004

[25] Tao H, Amsden JJ, Strikwerda AC, Fan K, Kaplan DL, Zhang X, Averitt RD, Omenetto FJ (2010) Metamaterial silk composites at terahertz frequencies. Adv. Mater. 22:3527–3531

[26] Chen ZC, Han NR, Pan ZY, Gong YD, Chong TC, Hong MH (2011) Tunable resonance enhancement of multi-layer terahertz metamaterials fabricated by parallel laser micro-lens array lithography on flexible substrates. Opt. Mat. Express 1:151-157

[27] Miyamaru F, Takeda MW, Taima K (2009) Characterization of terahertz metamaterials fabricated on flexible plastic films: toward fabrication of bulk metamaterials in terahertz region. Appl. Phys. Express 2:042001

[28] Peralta XG, Wanke MC, Arrington CL, Williams JD, Brener I, Strikwerda A, Averitt RD, Padilla WJ, Smirnova W, Taylor AJ, O'Hara FJ (2009) Large-area metamaterials on thin membranes for multilayer and curved applications at terahertz and higher frequencies. Appl. Phys. Lett. 94:161113

[29] Choi M, Lee SH, Kim Y, Kang SB, Shin J, Kwak MH, Kang KY, Lee YH, Park N, Min B (2011) A terahertz metamaterial with unnaturally high refractive index. Nature 470:369-373

[30] Han NR, Chen ZC, Lim CS, Ng B, Hong MH (2011) Broadband multi-layer terahertz metamaterials fabrication and characterization on flexible substrates. Opt. Express 19:6990-6998

[31] Aznabet M, Navarro-Cia N, Kuznetsov SA, Gelfand AV, Fedorinina NI, Goncharov YG, Beruete M, Mrabet OE, Sorolla M (2008) Polypropylene-substrate-based SRR- and CSRR-metasurfaces for submillimeter waves. Opt. Express 16:18312-18319

[32] Padilla WJ, Aronsson MT, Highstrete C, Lee M, Taylor AJ, Averitt RD (2007) Electrically resonant terahertz metamaterials: Theoretical and experimental investigations. Phys. Rev. B 75:041102(R)

[33] Chen HT, O'Hara FJ, Taylor AJ, Averitt RD, Highstrete C, Lee M, Padilla WJ (2007) Complementary planar terahertz metamaterials. Opt. Express 15:1084-1095

[34] Pendry JB, Holden AJ, Robbins DJ, Stewart WJ (1999) Magnetism from conductors and enhanced nonlinear phenomena. IEEE Trans. Microwave Theory Tech. 47:2075-2084